Chaotic Diffusion
and
Fractal Functions

Georgie Knight (079546195)
School of Mathematical Sciences
Queen Mary, University of London
Supervisor: Dr R. Klages

2008

Abstract

The idea of chaotic diffusion is briefly discussed, along with the definition of a diffusion coefficient. The Taylor-Green-Kubo formula is then derived, starting from Einstein's formula for diffusion in one dimension. This is then used to evaluate the diffusion coefficient for a lifted Bernoulli shift. The diffusion coefficient is obtained via the famous Takagi function, which is a continuous but nowhere differentiable fractal function, which can be calculated by solving a functional recursion relation. A parameter dependent version of the lifted Bernoulli shift map is considered, and again, the Taylor-Green-Kubo formula is used to calculate the diffusion coefficient. The structure of the diffusion coefficient is explained using a method based on Markov partitions.

Contents

1 Introduction

One-dimensional, chaotic dynamical systems can provide us with relatively simple examples for studying certain transport coefficients. In particular, given certain maps, an ensemble of points will seemingly spread out when they are iterated (see [9]). This spreading out is analogous to the physical phenomenon of diffusion, and appropriate diffusion coefficients can be obtained. In some parameter dependent maps, the diffusion coefficient has been found to be a fractal function of the parameter. One method in particular uses appropriate Taylor-Green-Kubo formulas, and certain fractal "Takagi" functions in order to obtain the parameter dependent diffusion coefficient (see [7]). The ultimate goal of this project is to apply this method to a lifted Bernoulli shift map, and hence obtain an exact, analytical expression for the diffusion coefficient, in terms of the lift parameter.

Firstly, in section 2, a brief outline of the idea of diffusion as a physical phenomenon will be given. This will be developed into the analogous case of diffusion in a purely mathematical context. The case of a random walk will be briefly discussed and then the idea of deterministic diffusion will be explained.

In section 3, the Taylor-Green-Kubo formula will be derived directly from Einstein's formula for diffusion. This formula is central to the method that will be used to obtain the diffusion coefficient. The Takagi function will be introduced as a constituent part of the Taylor-Green-Kubo formula. This formula will then be used to obtain a diffusion coefficient for a particular value of the parameter. This hopefully helps the reader (and the author) understand the process of obtaining the diffusion coefficient via the Taylor-Green-Kubo formula.

In section 4, the full, parameter dependent Takagi function will be derived and a necessary invariant density will be calculated. These two will be combined in the Taylor-Green-Kubo formula, to work out an expression for the parameter dependent diffusion coefficient. From this precise expression, very simple formulas for both large, and small values of the parameter will be derived.

Finally, in section 5, the fractal structure of the diffusion coefficient is explained by showing that there are certain classes of Markov partition that give the local extreme points of the diffusion coefficient.

2 Diffusion

2.1 Molecular Diffusion

From a purely physical perspective, diffusion is the process in which a system will move toward a state of concentration equilibrium, without any external influences like mixing. Diffusion causes a region of high concentration within a system to spread out, thereby diluting itself. As an illustration, one can imagine a drop of ink colouring an entire glass of water, without any mixing or turbulent motion within the water. The process of diffusion can be modeled by the partial differential equation,

$$\frac{\partial C}{\partial t} = D\frac{\partial^2 C}{\partial x^2} \quad . \tag{1}$$

This is a one-dimensional (one dimension will suffice in this project) version of the "diffusion equation" (see [5]). C is the concentration, t denotes time and x is our coordinate. D is a constant and is known as the "diffusion coefficient". This equation serves as a macroscopic definition of the diffusion coefficient. Eq.(1) can be derived from two simple equations. Firstly, the "continuity equation", given by,

$$\frac{\partial C}{\partial t} = -\frac{\partial F_x}{\partial x} \quad . \tag{2}$$

In Eq.(2), F_x is the "current density", or the number of molecules passing a point per unit time, in the x direction. Eq.(2) simply states that any rise or fall in concentration is caused by the movement of molecules into, or out of a region, respectively. Secondly, we need Fick's first law of diffusion, given by,

$$F_x = -D\frac{\partial C}{\partial x} \quad . \tag{3}$$

Fick's first law states that the current density is proportional to the concentration gradient. So a higher concentration gradient will result in a higher current density, and the change in current density is linear with respect to the change in concentration gradient. Note the minus sign; this indicates that the movement is from high to low concentration. By combining Eq.(2) and Eq.(3), Eq.(1) is recovered:

$$\begin{aligned} \frac{\partial C}{\partial t} &= -\frac{\partial}{\partial x}\left(-D\frac{\partial C}{\partial x}\right) \\ &= D\frac{\partial}{\partial x}\left(\frac{\partial C}{\partial x}\right) \\ &= D\frac{\partial^2 C}{\partial x^2} \quad . \end{aligned} \tag{4}$$

The diffusion coefficient in this physical example is a measure of how easily a molecule moves through it's given medium (e.g. how easily a drop of ink spreads out through water). By considering what is behind this process of molecular diffusion, we can build a more mathematical model.

The cause of molecular diffusion is the thermal energy associated with each molecule. This thermal energy causes each molecule to move randomly. Consequently, within a region of high concentration, a proportion of molecules will move out of the region, this results in diffusion (see [5]). We can now understand why a high concentration gradient results in a higher current density as it increases the probability of diffusive motion within a system. This understanding now leads us to develop more mathematical models of diffusion.

2.2 "Random Walk" Diffusion

Suppose we have a one-dimensional system in which a molecule moves positively or negatively a distance Δ with equal probability. Suppose further that this happens at discrete time intervals of length τ. This system is an example of a "random walk" (see [13]). The often given analogy is of a drunken sailor trying to make his way home from the bar (see [11]). This inebriated sailor is so far gone that he has no control of his movement and simply steps to the left or the right with equal probability (hence "random walk"). If our sailor, or our molecule, starts at a point $a\Delta$, what can we say about the probability of being found at $b\Delta$ given a time interval of $c\tau$? (a,b,$c \in N$).

We can say that the probability of being found at $b\Delta$ after a time interval of $(c+1)\tau$ relies on the neighbouring probabilities as follows, (see [13]):

$$P(b\Delta;(c+1)\tau \mid a\Delta) = \frac{1}{2}\left[P((b-1)\Delta;c\tau \mid a\Delta) + P((b+1)\Delta;c\tau \mid a\Delta)\right] \quad . \tag{5}$$

Eq.(5) simply states that the probability of being at $b\Delta$ after a time $(c+1)\tau$ is the sum of the probabilities of arriving at $b\Delta$ from the neighboring points. Eq.(5) can be rewritten by subtracting $P(b\Delta;c\tau \mid a\Delta)$ from both sides, dividing both sides by τ and multiplying the right hand side by Δ^2/Δ^2:

$$\frac{P(b\Delta;(c+1)\tau \mid a\Delta) - P(b\Delta;c\tau \mid a\Delta)}{\tau} =$$

$$\frac{\Delta^2}{2\tau}\left(\frac{[P((b-1)\Delta;c\tau \mid a\Delta) + P((b+1)\Delta;c\tau \mid a\Delta) - 2P(b\Delta;c\tau \mid a\Delta)}{\Delta^2}\right) \quad .$$

Now if we let Δ and τ go to zero, we get a familiar looking partial differential equation (see Eq.(1)):

$$\frac{\partial P}{\partial t} = D\frac{\partial^2 P}{\partial x^2} \quad . \tag{6}$$

So we see that a sailor undergoing a simple random walk, will actually experience a diffusive process. Hence, if we start with a whole crew of sailors, they will diffuse away from the bar over time. In this case, the diffusion coefficient $D = \Delta^2/2\tau$ is defined in terms of a microscopic interpretation. It is a special case of Einstein's formula (see [7]) for the diffusion coefficient:

$$D = \lim_{n\to\infty} \frac{\langle (x_n - x_0)^2 \rangle}{2n} \quad . \tag{7}$$

Here x_0 is the starting point and x_n is the distance from x_0 after n discrete time steps. The average is taken over the initial distribution of points. If we let $\Delta = 1$ and $\tau = 1$, we obtain a diffusion coefficient of,

$$D = \frac{1}{2} \quad . \tag{8}$$

2.3 Chaotic (Deterministic) Diffusion

Chaotic diffusion is found in some chaotic, dynamical systems. This project will focus on discrete-time. An ensemble of points in these systems, will diffuse away from their starting point over many time steps, and an appropriate diffusion coefficient can be derived. A simple case of chaotic diffusion, is found in one-dimensional, piecewise linear maps. The equations of motion are of the form,

$$x_{n+1} = M(x_n), \quad M : \Re \mapsto \Re, \quad x \in \Re, n \in N. \tag{9}$$

An important feature of these maps is that they are chaotic in the sense that they have "sensitive dependence on initial conditions" (see [1, 8]), i.e. small differences in initial conditions are amplified by iteration of the map. This causes an initial ensemble of points to spread out under iteration. This is crucial if we are going to define a diffusion coefficient for these maps. The defining feature of the diffusion in these maps, is that the position of a point x_0 at the n^{th} iteration is uniquely determined by the equations of motion given by Eq.(9). If we consider stochastic random walks, this is obviously not the case. A random walk is a "Markov" process, as each step is independent of the step that went before it. The random walk system has no memory. In chaotic diffusion, all of the motion is purely deterministic and hence we are studying deterministic diffusion. A particular example of chaotic diffusion is found in the lifted Bernoulli shift map. The main structure of the map is,

$$M_h(x) = \begin{cases} 2x + h & 0 \leq x < \frac{1}{2} \\ 2x - 1 - h & \frac{1}{2} \leq x < 1 \end{cases} \quad , 0 \leq x \leq 1 \quad . \tag{10}$$

Eq.(10) tells us how the map is defined on the unit interval and will be referred to as the "box" map. To create diffusion, the phase space will need to be sufficiently large. In our case, the phase space is the entire real line. To rigorously define this we have the condition,

$$M_h(x + 1) = M_h(x) + 1, \quad -\infty \leq x \leq \infty. \tag{11}$$

Eq.(11) takes the box map, copies it onto each unit interval, and raises or lowers it with a degree of one, so as to create a chain of boxes over the entire real line. This combination of a box map and a raising condition is a typical way to create a diffusive map (see [7]). The parameter h in Eq.(10) and Eq.(11) quantifies the lift condition, as it determines by how much the first piecewise branch of the box map is raised up from the x-axis, and by how much the second piecewise branch of the box map is lowered from the x-axis. We see that at

$h = 0$ the Bernoulli shift map is recovered, hence the term "lifted Bernoulli shift". Fig.(1) depicts the box map of Eq.(10) and the result of applying the raising condition of Eq.(11) to Eq.(10), and so gives a section of the map that will be studied in this project.

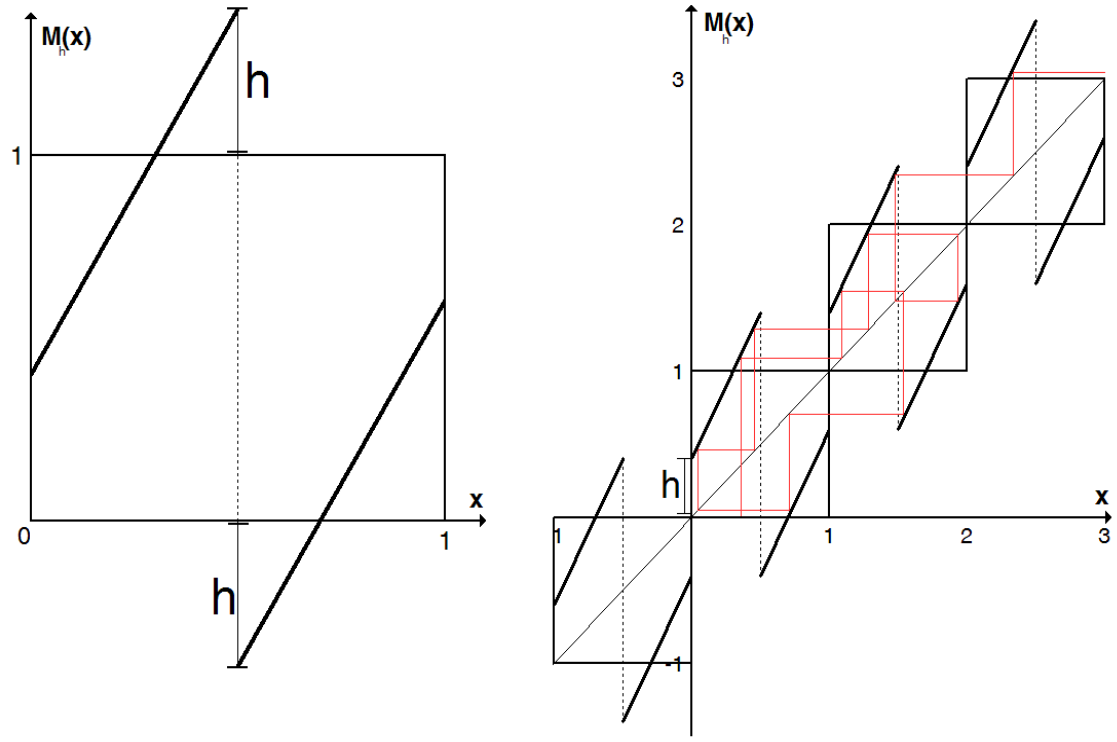

Figure 1: *The lifted Bernoulli shift map.* This figure depicts a section of the map that will be the focus of this project. The box map is on the left, and a section showing how the chain of boxes is constructed is on the right. Note that there are intervals where a point will move from one box to the next when iterated. This is necessary for diffusion. The orbit of such a point is included.

Now that we have our explicit equations of motion, we can quantify the spreading out of our initial ensemble of points via the "local Ljapunov exponent"; $\lambda(x_0)$, defined by,

$$\lambda(x_0) := \lim_{n\to\infty} \frac{1}{n} \sum_{i=0}^{n-1} \ln |M_h'(x_i)| \quad . \tag{12}$$

Here, x_0 is an initial point and x_i is the i^{th} iterate of x_0. $\lambda(x_0)$ is a measure of the rate of separation of two nearby points (see[8]). For the maps M_h, $\lambda(x_0) = \ln 2$ as $|M_h'(x_i)| = 2, (\forall x_0, \quad x_0 \neq 0.5)$. The positive Ljapunov exponent is a precise, mathematical measure of the "spreading out" of an initial ensemble of points.

3 The Taylor-Green-Kubo formula

3.1 Derivation

The Taylor-Green-Kubo formula (sometimes known as the Green-Kubo formula (see[2],[3],[7],[9])) can be used to obtain the diffusion coefficient for our map. Hence, it can be used to study the dependence of the diffusion coefficient on the parameter h. It can be derived straight from Eq.(7) (see [2]), along with the assumption that there exists an initial probability density distribution $\rho(x)$ that is invariant under the Frobenius-Perron equation (see [8]) given by,

$$\rho_{n+1}(x) = \sum_{x \in M(x^i)} \rho_n(x^i) \mid M'(x^i) \mid^{-1} \quad . \tag{13}$$

So we assume that there exists a $\rho^*(x)$ such that $\rho^*_{n+1}(x) = \rho^*_n(x)$. This is analogous to studying diffusion in a system that is in a state of equilibrium. This invariant density will be explicitly calculated in section 4. In addition, we need to define a "velocity" function that measures how far a point travels under one iteration. It is defined as,

$$\tilde{v}_j = \tilde{v}(x_j) := x_{j+1} - x_j \quad . \tag{14}$$

Remember that our diffusion coefficient D is given by Eq.(7) as follows:

$$\begin{aligned} D &= \lim_{n\to\infty} \frac{\langle (x_n - x_0)^2 \rangle}{2n} \\ &= \lim_{n\to\infty} \frac{1}{2n} \left\langle (x_n - x_{n-1} + x_{n-1} - x_{n-2} + x_{n-2} - x_{n-3} + ... - x_0)^2 \right\rangle \\ &= \lim_{n\to\infty} \frac{1}{2n} \left\langle \left(\sum_{j=0}^{n-1} \tilde{v}_j \right)^2 \right\rangle \quad . \end{aligned} \tag{15}$$

The average $\langle ... \rangle$ is taken over the points in our initial invariant density distribution. Continuing to evaluate the right hand side of Eq.(15) we find that,

$$\begin{aligned} D &= \lim_{n\to\infty} \frac{1}{2n} \left\langle (\tilde{v}_0 + \tilde{v}_1 + \tilde{v}_2 + ... + \tilde{v}_{n-1}) (\tilde{v}_0 + \tilde{v}_1 + \tilde{v}_2 + ... + \tilde{v}_{n-1}) \right\rangle \\ &= \lim_{n\to\infty} \frac{1}{2n} \left\langle \left(\sum_{j=0}^{n-1} (\tilde{v}_j)^2 + (\tilde{v}_0\tilde{v}_1 + \tilde{v}_0\tilde{v}_2 + ... + \tilde{v}_1\tilde{v}_0 + \tilde{v}_1\tilde{v}_2 + ... + \tilde{v}_{n-1}\tilde{v}_0 + \tilde{v}_{n-1}\tilde{v}_1 + ...) \right) \right\rangle \\ &= \lim_{n\to\infty} \frac{1}{2n} \left\langle \left(\sum_{j=0}^{n-1} (\tilde{v}_j)^2 + 2 \sum_{j \neq j'} \tilde{v}_j \tilde{v}_{j'} \right) \right\rangle \quad . \end{aligned} \tag{16}$$

Which can be simplified using the fact that the average is taken over an invariant density:

$$\begin{aligned} D &= \lim_{n\to\infty} \frac{1}{2n} \int_0^1 \rho^*(x) \left(\sum_{j=0}^{n-1} (\tilde{v}_j)^2 + 2 \sum_{j\neq j'} \tilde{v}_j \tilde{v}_{j'} \right) \quad dx \\ &= \lim_{n\to\infty} \frac{1}{2n} \left(\int_0^1 \rho^*(x) \sum_{j=0}^{n-1} (\tilde{v}_j)^2 \quad dx + \int_0^1 dx \rho^*(x) 2 \sum_{j\neq j'} \tilde{v}_j \tilde{v}_{j'} \quad dx \right) \\ &= \lim_{n\to\infty} \left(\frac{n}{2n} \int_0^1 \rho^*(x) (\tilde{v}_0)^2 \quad dx + \frac{2n}{2n} \sum_{k=1}^{\infty} \int_0^1 \rho^*(x) (\tilde{v}_k \tilde{v}_0) \quad dx \right) \\ &= \frac{1}{2} \left\langle \tilde{v}_0^2 \right\rangle + \sum_{k=1}^{\infty} \langle \tilde{v}_k \tilde{v}_0 \rangle \\ &= \sum_{k=0}^{\infty} \langle \tilde{v}_k \tilde{v}_0 \rangle - \frac{1}{2} \left\langle \tilde{v}_0^2 \right\rangle \end{aligned} \tag{17}$$

The important step is the use of an invariant density. We have $\rho_1^*(x) = \rho_2^*(x) = ... = \rho_n^*(x)$, as the density remains the same after each iteration of the map. We also have translational invariance such that $\langle v_m v_n \rangle = \langle v_{m-n} v_0 \rangle$. We can apply this translational invariance due to the invariant density. Eq.(17) can be simplified further by replacing the $\tilde{v}$ function with a much simpler function that measures how many boxes a point traverses under one iteration. (Where $\lfloor ... \rfloor$ denotes the "floor" function. So $\lfloor x \rfloor$ is the nearest integer $\leq x$):

$$v_j = v(x_j) := \lfloor x_{j+1} \rfloor - \lfloor x_j \rfloor \quad . \tag{18}$$

We can see that this substitution is possible if we let $\Delta x_n = x_n - x_0$ in Eq.(7), and further we let $\Delta x_n = \Delta X_n + \Delta \tilde{x}_n$. Where X_n is the integer part of the displacement and is therefore the part we are interested in and $\tilde{x}_n \in [0, 1)$ is the fractional part of the displacement:

$$\begin{aligned} D &= \lim_{n\to\infty} \frac{\langle (x_n - x_0)^2 \rangle}{2n} \\ &= \lim_{n\to\infty} \frac{\langle (\Delta x_n)^2 \rangle}{2n} \\ &= \lim_{n\to\infty} \frac{\langle (\Delta X_n + \Delta \tilde{x}_n)^2 \rangle}{2n} \\ &= \lim_{n\to\infty} \frac{\langle (\Delta X_n^2 + 2\Delta X_n \Delta \tilde{x}_n + \Delta \tilde{x}_n^2) \rangle}{2n} \quad . \end{aligned} \tag{19}$$

The second term in Eq.(19) is bounded by the "$Cauchy - Hölder \ \ inequality$", (see [10]) and the third term is also bounded, hence in the limit as n goes to infinity, only ΔX_n contributes to D. Using this result in Eq.(17), we derive the Taylor-Green-Kubo formula as,

$$
\begin{aligned}
D &= \lim_{n\to\infty} \frac{\langle (\Delta X_n)^2 \rangle}{2n} \\
&\vdots \\
&= \sum_{k=0}^{\infty} \langle v_k v_0 \rangle - \frac{1}{2} \left\langle v_0^2 \right\rangle \quad . \qquad (20)
\end{aligned}
$$

3.2 Using the formula

In order to illustrate the power of the Taylor-Green-Kubo formula, it will now be employed in a simple example where $h = 1$. Exactly the same calculation has been carried out in [2]. Fig.(2) below depicts a section of the corresponding map.

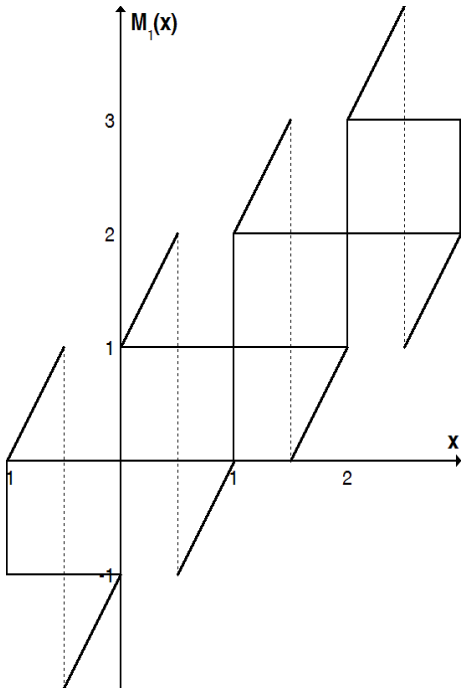

Figure 2: $M_1(x), x \in [-1, 3]$. This figure shows a section of the lifted Bernoulli shift map at a parameter value of $h = 1$. At each iteration, points move either to the left, or the right nearest box. So this map serves as a deterministic version for the random walk that was discussed earlier, in as much as a point picked at random will move to the left or the right at each time step.

The explicit equations of motion for the box map of $M_1(x)$ are given by,

$$M_1(x) = \begin{cases} 2x+1 & 0 \leq x < \frac{1}{2} \\ 2x-2 & \frac{1}{2} \leq x < 1 \end{cases} \quad , 0 \leq x \leq 1. \tag{21}$$

Hence, the velocity function for $M_1(x)$ is given by,

$$v(x_j) = \begin{cases} 1 & 0 \leq \tilde{x_j} < \frac{1}{2} \\ -1 & \frac{1}{2} \leq \tilde{x_j} < 1 \end{cases} \quad . \tag{22}$$

Where $\tilde{x} = x \bmod 1$. Secondly, we need to evaluate the invariant density $\rho^*(x)$ for our map. In order to do this we need only consider the reduced modulo 1 version of our map, $\tilde{M_1}(x)$, due to the condition of Eq.(11). In this case, $\tilde{M_1}(x)$ is simply the Bernoulli shift map, hence the invariant density is simply a constant function, i.e. $\rho^*(x) = 1$, (see [8]). So Eq.(20) can be expressed as,

$$D = \lim_{n\to\infty} \sum_{k=0}^{n} \int_0^1 v(x_0)v(x_k) \ \ dx - \frac{1}{2}\int_0^1 v^2(x_0) \ \ dx \ \ . \tag{23}$$

Following the method outlined in [2], the summation can be moved inside the integral in order to define a "Jump Function":

$$J_1^n(x_0) = \sum_{k=0}^{n} v(x_k) \ \ . \tag{24}$$

The jump function of Eq.(24) counts how many boxes an initial point is displaced by after n iterations. Due to the sensitive dependence on initial conditions, $J_1^n(x)$ will be a very badly behaved function for large n. So in order to work out D, we need to find a way to control $J_1^n(x)$. Firstly, we see that a recursion relation can be derived for $J_1^n(x)$:

$$\begin{aligned} J_1^n(x_0) &= \sum_{k=0}^{n} v\left(\tilde{M}_1^k(x_0)\right) \\ &= v(x_0) + \sum_{k=1}^{n} v\left(\tilde{M}_1^k(x_0)\right) \\ &= v(x_0) + J_1^{n-1}\left(\tilde{M}_1(x_0)\right) \ \ . \end{aligned} \tag{25}$$

Where again, $\tilde{M}_1(x) = M_1(x) \bmod 1$. The explicit equation for $\tilde{M}_1(x)$ is given by,

$$\tilde{M}_1(x) = \begin{cases} 2\tilde{x} & 0 \leq \tilde{x} < \frac{1}{2} \\ 2\tilde{x} - 1 & \frac{1}{2} \leq \tilde{x} < 1 \end{cases} \quad . \tag{26}$$

In order to manipulate $J_1^n(x)$, we integrate it in order to obtain a cumulative function $T_1^n(x)$ (see [3]):

$$\int J_1^n(x) \ \ dx = T_1^n(x) \ \ . \tag{27}$$

Using Eq.(25), and Eq.(27) we can derive a recursion relation for $T_1^n(x)$:

$$\begin{aligned} T_1^n(x) &= \int J_1^n(x) \ \ dx \\ &= \int v(x) + J_1^{n-1}\left(\tilde{M}_1(x)\right) \ \ dx \\ &= xv(x) + c + \frac{1}{2} T_1^{n-1}\left(\tilde{M}_1(x)\right) \\ &= t(x) + \frac{1}{2} T_1^{n-1}\left(\tilde{M}_1(x)\right) \ \ . \end{aligned} \tag{28}$$

Where $t(x) \equiv xv(x) + c$ and c is a constant function on each interval that $v(x)$ is constant. We can define c so that $T_1^n(x)$ is continuous on the interval [0,1] and $T_1^n(0) = T_1^n(1) = 0$. In order to be able to use $T_1^n(x)$, we need a more user friendly recursion relation. Via Eq.(22), and Eq.(26) we see that $J_1^n(x)$ is satisfied by,

$$J_1^n(x) = \begin{cases} 1 + J_1^{n-1}(2\tilde{x}) & 0 \leq \tilde{x} < \frac{1}{2} \\ -1 + J_1^{n-1}(2\tilde{x} - 1) & \frac{1}{2} \leq \tilde{x} < 1 \end{cases} \quad . \tag{29}$$

Integrating Eq.(29), we obtain a recursion relation for $T_1^n(x)$,

$$T_1^n(x) = \begin{cases} x + \frac{1}{2} T_1^{n-1}(2\tilde{x}) + c_1 & 0 \leq \tilde{x} < \frac{1}{2} \\ -x + \frac{1}{2} T_1^{n-1}(2\tilde{x} - 1) + c_2 & \frac{1}{2} \leq \tilde{x} < 1 \end{cases} , 0 \leq x \leq 1. \tag{30}$$

Applying the conditions that $T_1^n(0) = T_1^n(1) = 0$, we see that $c_1 = 0$ whilst $c_2 = 1$, and letting $n \to \infty$, we obtain the function $T_1(x)$:

$$T_1(x) = \begin{cases} x + \frac{1}{2} T_1(2\tilde{x}) & 0 \leq \tilde{x} < \frac{1}{2} \\ 1 - x + \frac{1}{2} T_1(2\tilde{x} - 1) & \frac{1}{2} \leq \tilde{x} < 1 \end{cases} , 0 \leq x \leq 1. \tag{31}$$

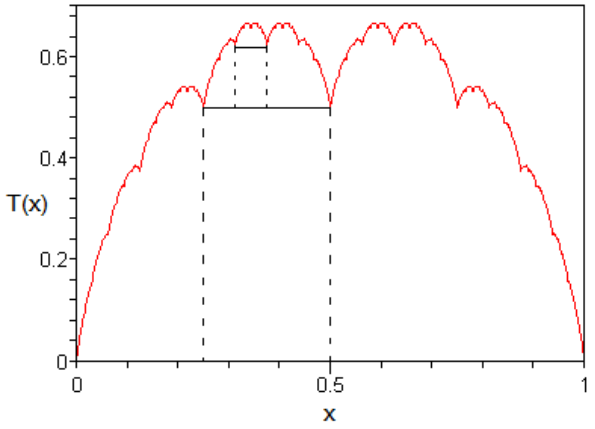

Figure 3: *The Takagi function.* In this figure the Takagi function for the parameter $h = 1$ is depicted. Takagi functions are characterised by being continuous but non-differentiable functions. Note the self similarity of the regions, $0.25 \leq x \leq 0.5$ and $0.5 \leq x \leq 0.75$ to the entire function. The dashed lines serve as a guide to this. (This image was created in *Maple 9.5* with 1024 data points. Each point is accurate to a value of $\pm\ 2^{-20}$ so that error bars are not visible.)

The function $T_1(x)$ is known as a *Takagi Function*. It is shown in Fig.(3). Using $T_1(x)$ in Eq.(23) we get,

$$\begin{aligned} D &= \int_0^1 v(x) J_1^n(x)\ \ dx - \frac{1}{2}\int_0^1 v^2(x)\ \ dx \\ &= \int_0^{\frac{1}{2}} v(x) J_1^n(x)\ \ dx + \int_{\frac{1}{2}}^1 v(x) J_1^n(x)\ \ dx - \frac{1}{2}\int_0^1 v^2(x)\ \ dx \\ &= [T_1(x)]_0^{\frac{1}{2}} - [T_1(x)]_{\frac{1}{2}}^1 - \frac{1}{2}[x]_0^1 \\ &= 2T\left(\frac{1}{2}\right) - T_1(0) - T_1(1) - \frac{1}{2} \\ &= \mathbf{\frac{1}{2}}\ . \end{aligned}$$

This value of D corresponds to the result obtained in Eq.(8) and shows how the deterministic system is analogous to the stochastic one of the random walk, at this value of the parameter. We can also set the parameter $h = 0$. Obviously in this system there is no diffusion, as there is no escape between boxes. In terms of evaluating D with our method, we see that the velocity function $v(x) = 0\ \ \forall x$. Hence Eq.(23) gives a value of 0 for D. The method outlined here, although complicated, can be employed in less trivial, more general examples (see [7]).

4 Parameter Dependence

4.1 Takagi Function

In the previous section, it was shown that the diffusion coefficient for M_h is equal to 0 when $h = 0$, and is equal to $\frac{1}{2}$ when $h = 1$. One may now ask what happens to the diffusion coefficient as h is changed? Intuitively, it seems reasonable to guess that D increases linearly. However, approximate calculations in different maps, but similar parameter, (see [7]) show that for small values of h, the increase is linear whereas for large values the increase is quadratic. In addition, the diffusion coefficient is shown to be a fractal function of the parameter. Precise results via a different method (see [4]) also display this fractal behaviour.

When evaluating the parameter dependent diffusion coefficient, there are two main obstacles. Firstly, the Takagi function will need to be evaluated in terms of h. Secondly, the invariant density will need to be calculated with respect to h. To evaluate the Takagi function we need to start with the velocity function $v_h(x)$ for $x \in [0, 1]$. This is given by,

$$v_h(x) = \begin{cases} \lfloor h \rfloor & 0 \leq \tilde{x} < \frac{1-\hat{h}}{2} \\ \lceil h \rceil & \frac{1-\hat{h}}{2} \leq \tilde{x} < \frac{1}{2} \\ -\lceil h \rceil & \frac{1}{2} \leq \tilde{x} < \frac{1+\hat{h}}{2} \\ -\lfloor h \rfloor & \frac{1+\hat{h}}{2} \leq \tilde{x} < 1 \end{cases} . \tag{32}$$

The function $\hat{h}$ is similar to $h \bmod 1$ except it takes the value 1 for all integer values of h except 0 where it takes the value 0. This is in order to represent the intervals correctly as h is varied. Eq.(32) leads to the evaluation of the parameter dependent jump function $J_h^n(x)$:

$$J_h^n(x) = \begin{cases} \lfloor h \rfloor + J_h^{n-1}\left(\tilde{M}_h(x)\right) & 0 \leq \tilde{x} < \frac{1-\hat{h}}{2} \\ \lceil h \rceil + J_h^{n-1}\left(\tilde{M}_h(x)\right) & \frac{1-\hat{h}}{2} \leq \tilde{x} < \frac{1}{2} \\ -\lceil h \rceil + J_h^{n-1}\left(\tilde{M}_h(x)\right) & \frac{1}{2} \leq \tilde{x} < \frac{1+\hat{h}}{2} \\ -\lfloor h \rfloor + J_h^{n-1}\left(\tilde{M}_h(x)\right) & \frac{1+\hat{h}}{2} \leq \tilde{x} < 1 \end{cases} . \tag{33}$$

Again, $\tilde{M}_h(x) = M_h(x) \bmod 1$, it is given by,

$$\tilde{M}_h(x) = \begin{cases} 2\tilde{x} + \hat{h} & 0 \leq \tilde{x} < \frac{1-\hat{h}}{2} \\ 2\tilde{x} + \hat{h} - 1 & \frac{1-\hat{h}}{2} \leq \tilde{x} < \frac{1}{2} \\ 2\tilde{x} - \hat{h} & \frac{1}{2} \leq \tilde{x} < \frac{1+\hat{h}}{2} \\ 2\tilde{x} - 1 - \hat{h} & \frac{1+\hat{h}}{2} \leq \tilde{x} < 1 \end{cases} . \tag{34}$$

By integrating Eq.(33), we can begin to evaluate the parameter dependent Takagi function, that we need in order to find the diffusion coefficient.

$$T_h^n(x) = \begin{cases} \frac{1}{2}T_h^{n-1}\left(2\tilde{x}+\hat{h}\right) + c_1 + \lfloor h \rfloor \tilde{x} & 0 \le \tilde{x} < \frac{1-\hat{h}}{2} \\ \frac{1}{2}T_h^{n-1}\left(2\tilde{x}+\hat{h}-1\right) + c_2 + \lceil h \rceil \tilde{x} & \frac{1-\hat{h}}{2} \le \tilde{x} < \frac{1}{2} \\ \frac{1}{2}T_h^{n-1}\left(2\tilde{x}-\hat{h}\right) + c_3 - \lceil h \rceil \tilde{x} & \frac{1}{2} \le \tilde{x} < \frac{1+\hat{h}}{2} \\ \frac{1}{2}T_h^{n-1}\left(2\tilde{x}-1-\hat{h}\right) + c_4 - \lfloor h \rfloor \tilde{x} & \frac{1+\hat{h}}{2} \le \tilde{x} \le 1 \end{cases}, 0 \le x \le 1. \quad (35)$$

Again, we can use the conditions that $T_h^n(0) = T_h^n(1) = 0$, and also that the function should be continuous in order to evaluate the constants of integration. We also use the symmetry of the Takagi functions to simplify the results. If we use these conditions and let $n \to \infty$, the following relations are obtained:

1. $T_h(0) = \frac{1}{2}T_h(\hat{h}) + c_1 = 0$
2. $T_h(1) = \frac{1}{2}T_h(\hat{h}) + c_4 - \lfloor h \rfloor = 0$
3. $T_h\left(\frac{1-\hat{h}}{2}\right) = \frac{1}{2}T_h(0) + c_2 + \lceil h \rceil \left(\frac{1-\hat{h}}{2}\right)$
4. $T_h\left(\frac{1-\hat{h}}{2}\right) = \frac{1}{2}T_h(1) + c_1 + \lfloor h \rfloor \left(\frac{1-\hat{h}}{2}\right)$
5. $T_h\left(\frac{1}{2}\right) = \frac{1}{2}T_h(\hat{h}) + c_2 + \lceil h \rceil \frac{1}{2}$
6. $T_h\left(\frac{1}{2}\right) = \frac{1}{2}T_h(1-\hat{h}) + c_3 - \lfloor h \rfloor \frac{1}{2}$
7. $T_h\left(\frac{1+\hat{h}}{2}\right) = \frac{1}{2}T_h(1) + c_3 - \lfloor h \rfloor \left(\frac{1+\hat{h}}{2}\right)$
8. $T_h\left(\frac{1+\hat{h}}{2}\right) = \frac{1}{2}T_h(0) + c_4 - \lfloor h \rfloor \left(\frac{1+\hat{h}}{2}\right)$

These results furnish us with the constants of integration and we obtain the Takagi function in terms of the parameter:

$$T_h(x) = \begin{cases} \frac{1}{2}T_h\left(2\tilde{x}+\hat{h}\right) + \lfloor h \rfloor \tilde{x} - \frac{1}{2}T_h(\hat{h}) & 0 \le \tilde{x} < \frac{1-\hat{h}}{2} \\ \frac{1}{2}T_h\left(2\tilde{x}+\hat{h}-1\right) + \lceil h \rceil \tilde{x} + \frac{\hat{h}-1}{2} - \frac{1}{2}T_h(\hat{h}) & \frac{1-\hat{h}}{2} \le \tilde{x} < \frac{1}{2} \\ \frac{1}{2}T_h\left(2\tilde{x}-\hat{h}\right) + \frac{1+\hat{h}}{2} - \lceil h \rceil \tilde{x} - \frac{1}{2}T_h(\hat{h}) & \frac{1}{2} \le \tilde{x} < \frac{1+\hat{h}}{2} \\ \frac{1}{2}T_h\left(2\tilde{x}-1-\hat{h}\right) - \lfloor h \rfloor \tilde{x} + \lfloor h \rfloor - \frac{1}{2}T_h(\hat{h}) & \frac{1+\hat{h}}{2} \le \tilde{x} \le 1 \end{cases}, 0 \le x \le 1. \quad (36)$$

Fig.(4) and Fig.(5) overleaf depict Eq.(36) at some particular values of h.

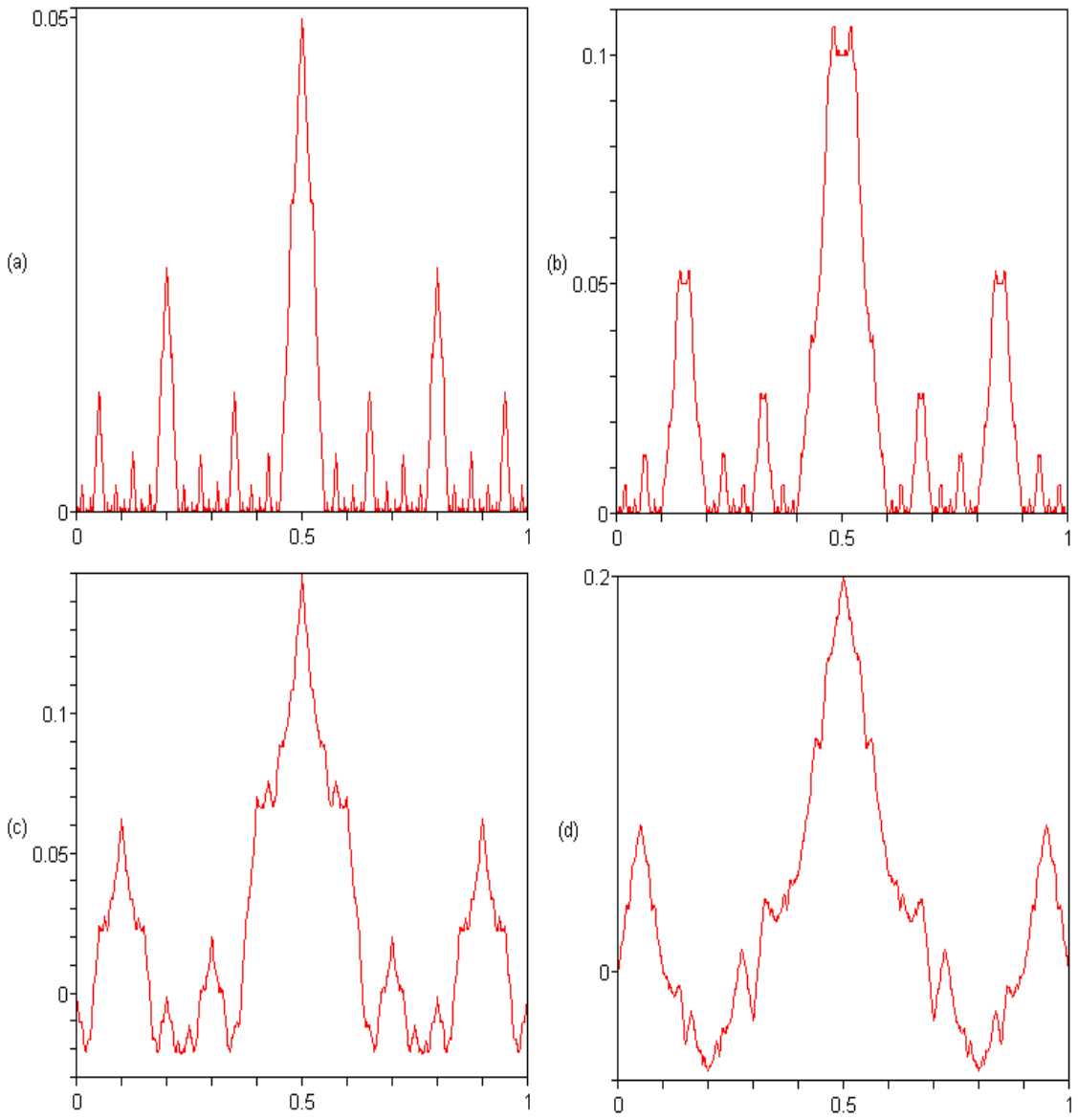

Figure 4: *Takagi functions for values of* $h < 0.5$. In this figure, Takagi functions have been plotted for the value $h = 0.1$ in (a), $h = 0.2$ in (b), $h = 0.3$ in (c) and $h = 0.4$ in (d). For each value of x, the Takagi function sums up all of the jumps that every point $\leq x$ has performed when $M_h(x)$ has been iterated an infinite amount of times. Hence, these fantastic functions have a fractal structure, which is a consequence of $M_h(x)$ being chaotic. These snapshots of the function give an idea of how the Takagi function grows as h increases. Notice how the function bifurcates as it grows. (These images were created in *Maple 9.5* with 1024 data points. Each point is accurate to a value of $\pm\ 2^{-20}$ so that error bars are not visible.)

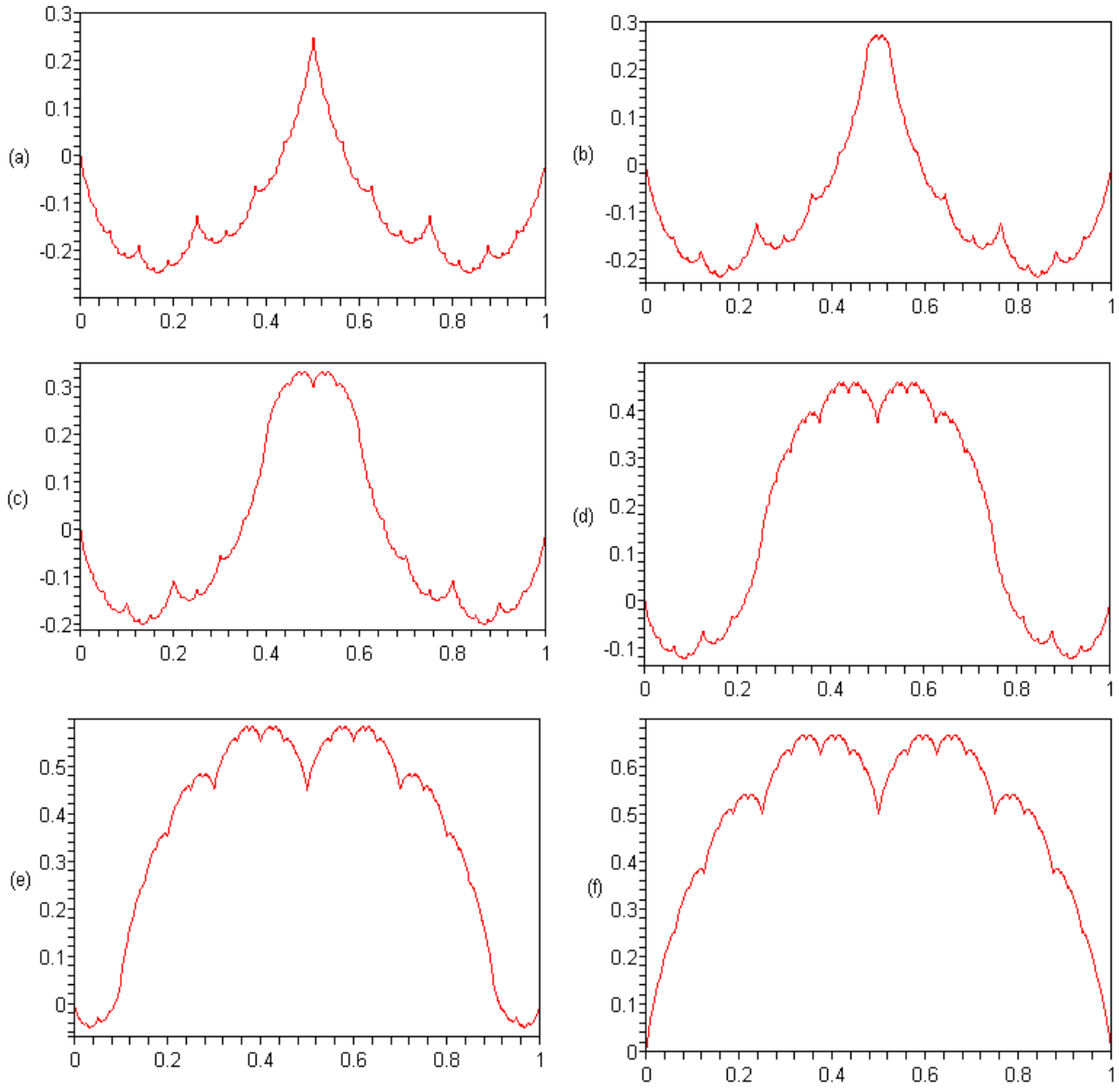

Figure 5: *Takagi functions for values of* $h > 0.5$. In this figure, Takagi functions have been plotted for the value $h = 0.5$ in (a), $h = 0.525$ in (b), $h = 0.6$ in (c), $h = 0.7$ in (d),$h = 0.9$ in (e) and $h = 1$ in (f). Notice again the fractal structure. In this range of values, the snapshots make it very clear how the Takagi function grows as h increases. The function goes through a process similar to inversion as it grows. Note that the Takagi functions for this map have negative regions. This is typically not the case for Takagi functions, (see [7]). (These images were created in *Maple 9.5* with 1024 data points. Each point is accurate to a value of $\pm\ 2^{-20}$ so that error bars are not visible.)

In order to evaluate Eq.(36) numerically, we can use the recurrence relation, (see [7]),

$$T_h(x) = \lim_{n\to\infty} T_h^n(x) = t_h(x) + \frac{1}{2}T_h^{n-1}\left(\tilde{M}_h(x)\right) \quad . \tag{37}$$

If we continue to apply this recursion relation we obtain the following summation:

$$T_h(x) = \lim_{n\to\infty} T_h^n(x) = -T_h(\hat{h}) + \sum_{k=0}^{\infty} \frac{1}{2^k} t_h\left(\tilde{M}_h^k(x)\right) \quad . \tag{38}$$

Where $T_h(\hat{h})$ has been summed separately, and $t_h(x)$ is as follows:

$$t_h(x) = \begin{cases} \lfloor h \rfloor \tilde{x} & 0 \le \tilde{x} < \frac{1-\hat{h}}{2} \\ \frac{\hat{h}-1}{2} + \lceil h \rceil \tilde{x} & \frac{1-\hat{h}}{2} \le \tilde{x} < \frac{1}{2} \\ \frac{1+\hat{h}}{2} - \lceil h \rceil \tilde{x} & \frac{1}{2} \le \tilde{x} < \frac{1+\hat{h}}{2} \\ \lfloor h \rfloor - \lfloor h \rfloor \tilde{x} & \frac{1+\hat{h}}{2} \le \tilde{x} < 1 \end{cases} \quad . \tag{39}$$

Note that Eq.(39) is simply Eq.(36) with all the Takagi functions removed. So Eq.(38) gives us a way to evaluate Takagi functions without using Takagi functions. Now that we have a parameter dependent Takagi function, we need the invariant density.

4.2 Invariant Density

In order to evaluate the invariant density, we need to solve the Frobenius-Perron equation, Eq.(13). To keep the calculations simple, we need only consider the invariant density for $\tilde{M}_h(x)$, Eq.(34). Obviously, $\tilde{M}_h'(x) = 2, \forall x$ except at the points of discontinuity. To construct the Frobenius-Perron equation for $\tilde{M}_h(x)$, we need to piecewise invert the function (see Fig.(6)). The following results are obtained for $h \le \frac{1}{2}$, a similar calculation can be made for $h \ge \frac{1}{2}$:

$$\begin{aligned} x_3 &= \frac{x-h+1}{2} && 0 \le \tilde{M}_h(x) < h \\ x_5 &= \frac{x+h+1}{2} && 0 \le \tilde{M}_h(x) < h \\ x_1 &= \frac{x-h}{2} && h \le \tilde{M}_h(x) < 1-h \\ x_6 &= \frac{x+h+1}{2} && h \le \tilde{M}_h(x) < 1-h \\ x_2 &= \frac{x-h}{2} && 1-h \le \tilde{M}_h(x) < 1 \\ x_4 &= \frac{x+h}{2} && 1-h \le \tilde{M}_h(x) < 1 \end{aligned} \tag{40}$$

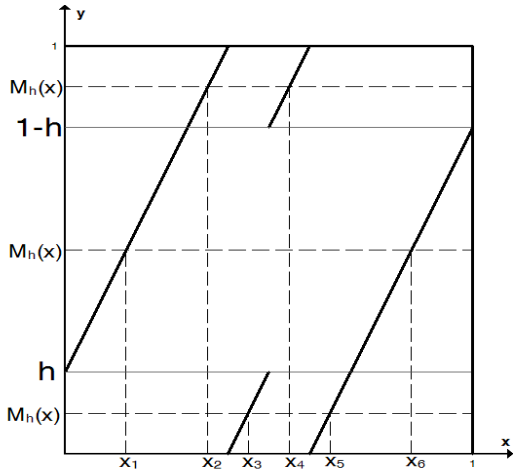

Figure 6: *Piecewise inverting $\tilde{M}_h(x)$ for a given value of h.* The dashed lines in this figure show how the pre-images of $\tilde{M}_h(x)$ are obtained.

Eq.(40) gives us the following Frobenius-Perron equation:

$$\rho_{n+1}(x) = \begin{cases} \frac{1}{2}\rho_n(\frac{x-h+1}{2}) + \frac{1}{2}\rho_n(\frac{x+h+1}{2}) & 0 \leq \tilde{M}_h(x) < h \\ \frac{1}{2}\rho_n(\frac{x-h}{2}) + \frac{1}{2}\rho_n(\frac{x+h+1}{2}) & h \leq \tilde{M}_h(x) < 1-h \\ \frac{1}{2}\rho_n(\frac{x-h}{2}) + \frac{1}{2}\rho_n(\frac{x+h}{2}) & 1-h \leq \tilde{M}_h(x) < 1 \end{cases} \tag{41}$$

We can make an educated guess that the invariant density $\rho^*(x)$ is uniform for the map $\tilde{M}_h(x)$. This is simply based on the fact that the invariant density is uniform for the Bernoulli shift map ($x_{n+1} = 2x \bmod 1$), which is recovered when $h = 0$. It can be quickly verified from Eq.(41) that the invariant density is uniform, and hence does not depend upon h. This will greatly simplify the calculation of the Diffusion Coefficient.

4.3 Diffusion Coefficient

Now we have the Takagi function given by Eq.(36), and we know that the invariant density is a constant function for all values of h. We can now combine these two ingredients in the Taylor-Green-Kubo formula of Eq.(20) and evaluate the parameter dependent diffusion coefficient:

$$
\begin{aligned}
D(h) &= \int_0^1 v_h(x) J_h^n(x)\ dx - \frac{1}{2}\int_0^1 v_h^2(x)\ dx \\
&= \int_0^{\frac{1-\hat{h}}{2}} \lfloor h \rfloor\, J_h^n(x)\ dx + \int_{\frac{1-\hat{h}}{2}}^{\frac{1}{2}} \lceil h \rceil\, J_h^n(x)\ dx + \int_{\frac{1}{2}}^{\frac{1+\hat{h}}{2}} \lceil h \rceil\, J_h^n(x)\ dx \\
&- \int_{\frac{1+\hat{h}}{2}}^1 \lfloor h \rfloor\, J_h^n(x)\ dx - \frac{1}{2}\left(\int_0^{\frac{1-\hat{h}}{2}} \lfloor h \rfloor^2 + \int_{\frac{1-\hat{h}}{2}}^{\frac{1}{2}} \lceil h \rceil^2 + \int_{\frac{1}{2}}^{\frac{1+\hat{h}}{2}} \lceil h \rceil^2 + \int_{\frac{1+\hat{h}}{2}}^1 \lfloor h \rfloor^2 \right) \\
&= \left(\lfloor h \rfloor - \lceil h \rceil\right)\left(\lfloor h \rfloor - \hat{h}\,\lfloor h \rfloor - T_h\left(\hat{h}\right)\right) + \lceil h \rceil\left(\lceil h \rceil + \hat{h} - 1\right) \\
&- \frac{1}{2}\left(\lfloor h \rfloor^2\left(1-\hat{h}\right) + \lceil h \rceil^2\,\hat{h}\right) \\
&= \left(\lfloor h \rfloor - \lceil h \rceil\right)^2\left(\frac{1}{2} - \frac{\hat{h}}{2}\right) + \frac{\lceil h \rceil^2}{2} + \lceil h \rceil\left(\hat{h} - 1\right) - \left(\lfloor h \rfloor - \lceil h \rceil\right) T_h\left(\hat{h}\right) \\
&= \frac{\lceil h \rceil^2}{2} + \left(\frac{1-\hat{h}}{2}\right)\left(1 - 2\lceil h \rceil\right) + T_h\left(\hat{h}\right) \quad . \qquad (42)
\end{aligned}
$$

Eq.(42) gives the exact, analytical expression for the diffusion coefficient, in terms of h, that was the goal of this project. The first two terms in Eq.(42) form a piecewise linear function that resembles $\frac{h^2}{2}$ for large h. See Fig.(7) below for a plot of Eq.(42).

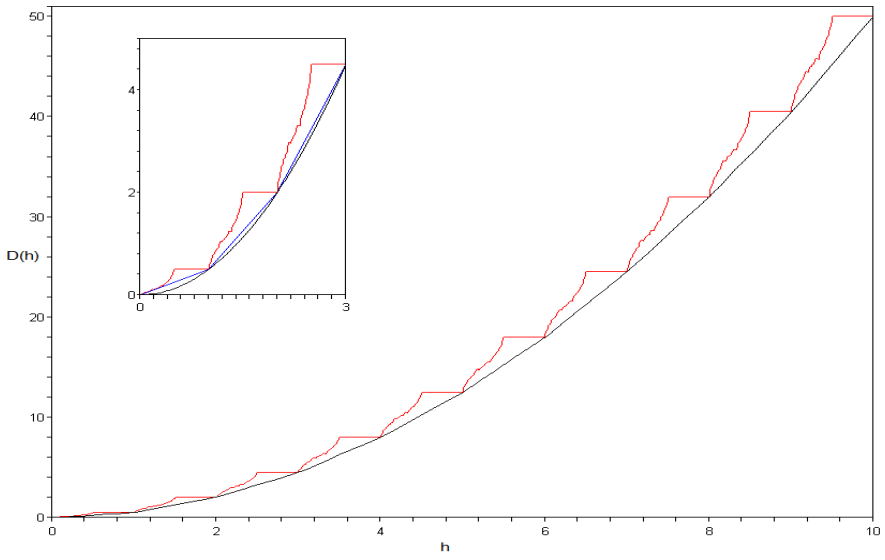

Figure 7: *The parameter dependent diffusion coefficient.* In this figure the diffusion coefficient is plotted along with $\frac{h^2}{2}$. Note the periodic pattern. The inset also gives the piecewise linear function, it shows how all three functions are incident at integer vales. (This image was created using *Maple 9.5*).

Given that the piecewise function in Eq.(42), closely resembles the function $\frac{h^2}{2}$, a good approximation of $D(h)$ for large h is the simple formula,

$$D(h) \approx \frac{h^2}{2} + T_h\left(\hat{h}\right) \quad h >> 0 \quad . \tag{43}$$

We also know that $T_h(x) = 0$ for integer values of x, so a formula for $D(h)$ at integer values of h is simply,

$$D(h) = \frac{h^2}{2}, \quad h \in Z. \tag{44}$$

If h is restricted to values in the range $[0, 1]$ then Eq.(42) is simplified, and a precise formula for evaluating $D(h)$ is,

$$D(h) = \frac{h}{2} + T_h(h) \quad 0 \leq h \leq 1 \quad . \tag{45}$$

Eqs.(42 – 45), give simple, useful formulas for evaluating the diffusion coefficient. Eq.(45) in particular highlights the important feature of deterministic diffusion. We see that there is an element of stochasticity that is found in a random walk, given by the term $\frac{h}{2}$. However the Takagi function gives the history of the initial ensemble of points, as it sums up all of the jump velocities. This is the deterministic element in the diffusion coefficient. Furthermore we can immediately see that by setting $h = 1$ or $h = 0$, our previous results that $D = \frac{1}{2}$ and $D = 0$ respectively are recovered.

5 The Structure of $D(h)$

Globally, we observe an increase in the diffusion coefficient as h increases. This is due to the corresponding increase in the velocity functions (Eq.(32)). However, the increase is far from straight forward. Fig.(7) shows the periodic pattern of $D(h)$ in which the regions where,

$$n \leq h \leq n + 0.5, \quad n \in N, \tag{46}$$

show a fractal structure. Whereas, the regions where,

$$n + 0.5 \leq h \leq n + 1, \quad n \in N, \tag{47}$$

show that $D(h)$ goes through a plateau. In order to explain these results, we can not resort to the calculus to obtain the turning points of $D(h)$. The Takagi functions are not differentiable, and so do not warrant this approach. Instead, an approach based upon the Markov partitions of $M_h(x)$, will give us some information about the structure of the diffusion coefficient. This follows the method used in [7]. Briefly, a partition of an interval is called Markov, when parts of the partition are mapped onto parts, or a union of parts of the partition (see [8]). Therefore, a Markov partition can tell us how a density of points behaves when iterated, and tells us about the topology of the map.

Firstly, we need only consider $\tilde{M}_h(x)$, given by Eq.(34), in order to construct Markov partitions for the entire map. This is due to the condition given by Eq.(11). This gives our first explanation of one of the characteristic features of the diffusion coefficient. The periodic scaling. Fig.(7) shows this in the pattern of the diffusion coefficient. While $\tilde{M}_h(x)$ is periodic, the velocity functions given by Eq.(32) increase regularly. Hence, the only difference in the diffusion coefficient of points that are equal modulo 1, is given by the scaling up of the velocity function.

In order to explain the structure of $D(h)$ more fully, we find certain classes of Markov partition for particular values of h. One class gives highly diffusive behaviour, and hence gives a local maximum. One restricts diffusion, and hence gives a local minimum.

When constructing a Markov partition for the map, we consider a point of discontinuity (e.g $x = 0.5$) and look at it's orbit. As parts of a Markov partition must get mapped onto parts of the partition, if $x = 0.5$ is a partition point then $M_h(0.5)$ must also be a partition point.

In addition, due to the central symmetry of $M_h(x)$, $(1 - M_h(0.5))$ must also be a partition point. Each iteration of the point $x = 0.5$ gives a partition point. Fig.(8) shows this process.

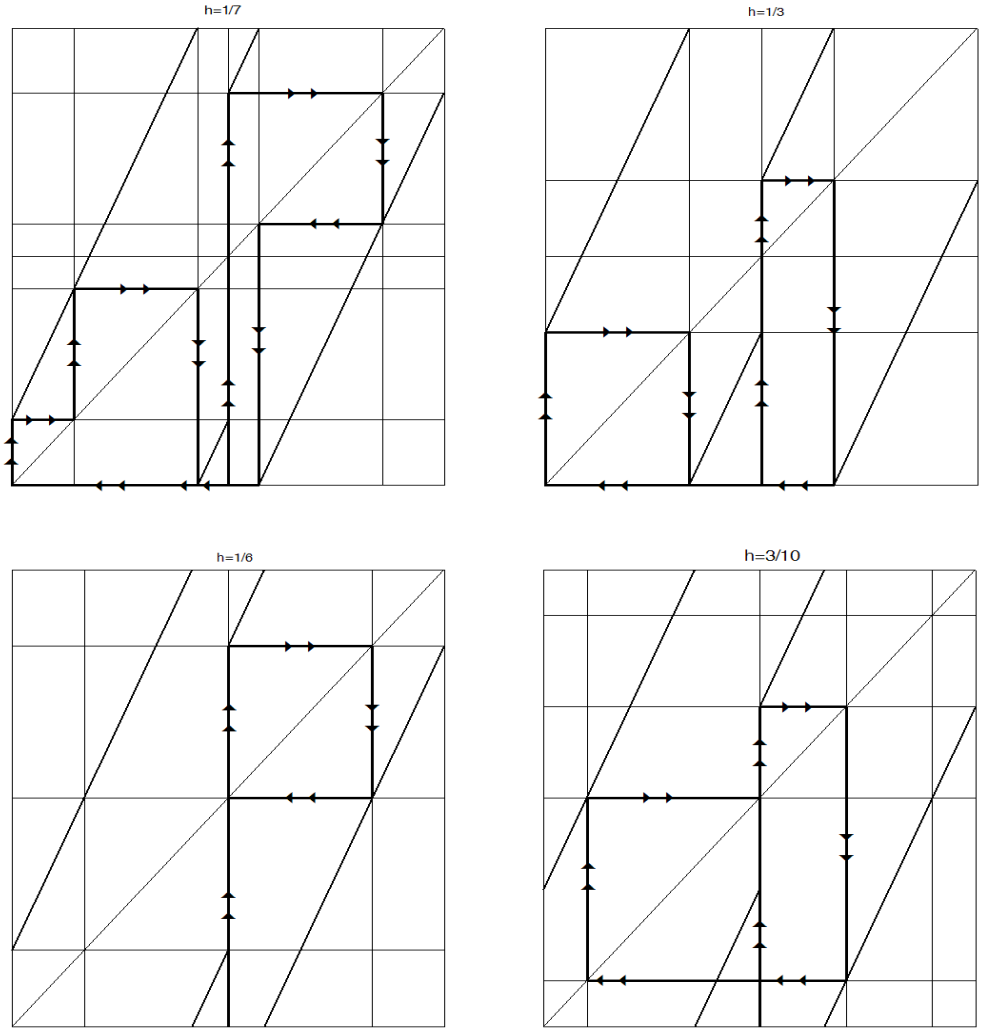

Figure 8: *Generating Markov partitions.* This figure shows how the orbit of the point $x = 0.5$ can generate a Markov partition of the unit interval. This process ends when the orbit is mapped onto itself, so the partitions can be very complex, depending on the periodicity of $x = 0.5$. Hence the partitions can have any number of parts.

If we restrict the values of h to $0.5 \leq h \leq 1$, we get an explanation for the plateau regions of $D(h)$. We see that,

$$\begin{aligned} \tilde{M}_h(0.5) &= 2(0.5) - h \\ &= 1 - h \quad . \end{aligned} \tag{48}$$

Eq.(48) holds for all values of h and has two consequences. One is that $1 - h$ is a partition point, the other is that h is a partition point. Furthermore, strictly for $0.5 \leq h \leq 1$ we see that,

$$\begin{aligned} \tilde{M}_h(1-h) &= 2(1-h) + h - 1, \quad 0.5 \leq h \leq 1 \\ &= 1 - h \quad . \end{aligned} \tag{49}$$

In addition, we find that,

$$\begin{aligned} \tilde{M}_h(h) &= 2(h) - h, \quad 0.5 \leq h < 1 \\ &= h \quad . \end{aligned} \tag{50}$$

Eqs.(49,50) show that h and $1 - h$ are fixed points of $\tilde{M}_h(x)$ and so for $0.5 \leq h \leq 1$ there are no more partition parts and the topology of $\tilde{M}_h(x)$ does not change. This results in the plateau regions. This behaviour is also mirrored in the Takagi functions. Fig.(4) shows some Takagi functions for $0 < h < 0.5$, whilst Fig.(5) shows some Takagi functions for $0.5 \leq h \leq 1$. We see in the latter, that there is a very smooth transition as h increases, the function inverts itself. Whereas in the former the function experiences a series of bifurcations as it grows.

The region where $0 \leq h < 0.5$, is more complicated, a first look tells us that there are many turning points in $D(h)$. See Fig.(9). We can use the behaviour of the Markov partitions to elucidate some information about these extrema. The local maximums must correspond to values of h where points jump from one interval to the next easily, and local minimums represent the opposite.

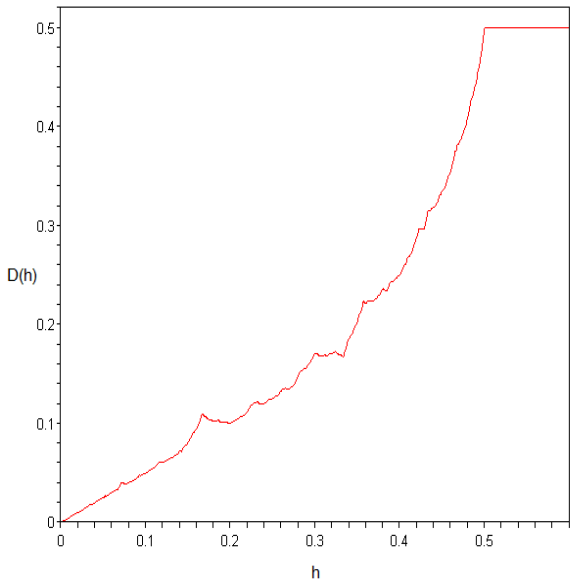

Figure 9: *Detail of the fractal region of $D(h)$.* This figure shows the diffusion coefficient for a lifted Bernoulli shift map. We see that the diffusion coefficient is a fractal function of the parameter in this region.

In the process of creating Markov partitions for a given value of h, we iterate the point $x = 0.5$ and the orbit of this point gives the rest of the partition points. If $x = 0.5$ were to be mapped onto itself, this would give a very simple Markov partition, and also a continually escaping orbit. Continually escaping in that at each iteration of the map it moves from one box to the next and so keeps moving away from it's starting point. After n iterations of the map, it will be n boxes from it's starting box. It would also mean that points nearby $x = 0.5$ would have similar trajectories to start with. Consequently, we would see a local maximum in $D(h)$.

$$\begin{aligned} \tilde{M}_h(0.5) &= 0.5 \\ 1 - h &= 0.5 \\ h &= 0.5 \quad . \end{aligned} \tag{51}$$

Eq.(51) gives the value of h that will give us the desired topology and the desired local maximum. If we evaluate,

$$\tilde{M}_h^2(0.5) = 0.5 \quad , \tag{52}$$

we will obtain a value of h that will give us similar topology to when $h = 0.5$. Hence we expect to obtain a value of h at which we will have a level 2 local maximum. "Level 2"

because it corresponds to a maximum where 0.5 is periodic with period 2. When evaluating Eq.(52), we obtain two different solutions for h. This is due to the different branches of $\tilde{M}_h(x)$. For $(0 \leq h \leq \frac{1}{3})$ we find,

$$\begin{aligned} \tilde{M}_h^2(0.5) &= 0.5 \\ \tilde{M}_h(1-h) &= 0.5 \\ 2-2h-1-h &= 0.5 \\ 0.5 &= 3h \\ h &= \frac{1}{6} \quad . \end{aligned} \tag{53}$$

For $\frac{1}{3} \leq h \leq 0.5$, we recover the value $h = 0.5$ as a solution. For comparison, the orbits of $x = 0.5$ at $h = 0.5$ and $h = \frac{1}{6}$ are shown in Fig.(10):

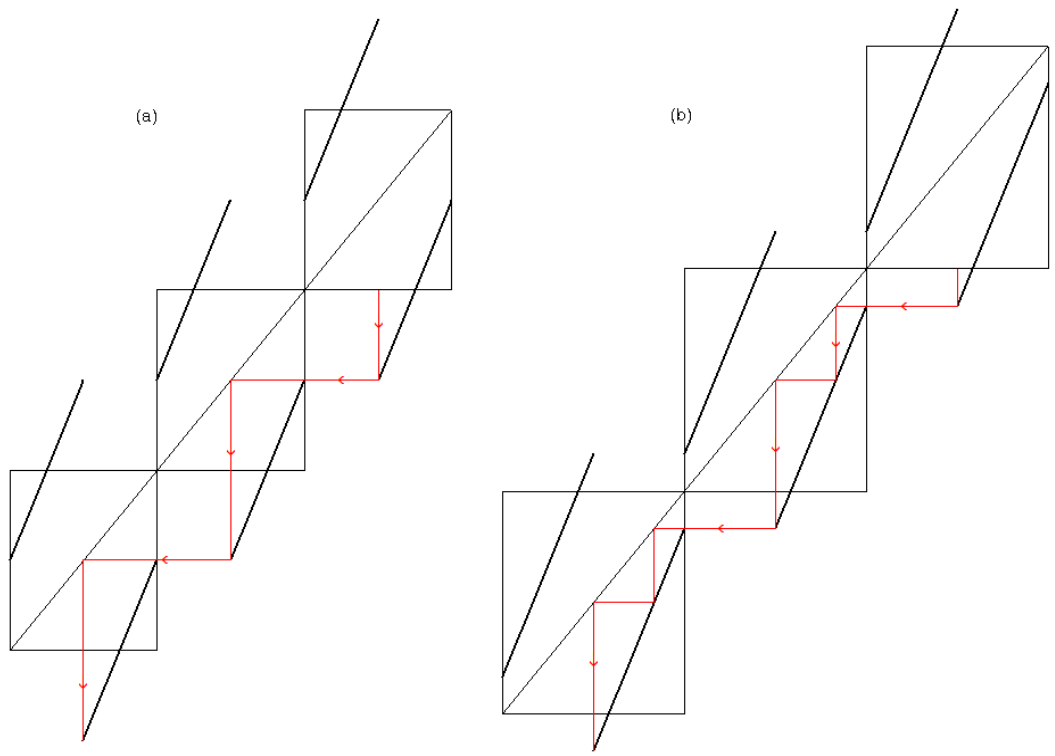

Figure 10: *The orbit of* $x = 0.5$ *for* $h = 0.5$ *in (a) and* $h = \frac{1}{6}$ *in (b).* Both orbits in (a) and (b) move steadily away from the point $x = 0.5$. However, after $2n$ iterations, the orbit in (a) will be a distance $2n$ from 0.5, in (b) it will only be a distance n.

For the minimums of $D(h)$, we need to see the orbit of $x = 0.5$ hit the point $x = \frac{1+h}{2}$. This results in an orbit that gets sent back, rather than continuing to travel away from it's starting point.

$$\begin{aligned} \tilde{M}_h(0.5) &= \frac{1+h}{2} \\ 1-h &= \frac{1+h}{2} \\ h &= \frac{1}{3} \quad . \end{aligned} \tag{54}$$

Eq.(54) tells us that the desired value is $h = \frac{1}{3}$, and Fig.(11) shows that the orbit of this point is eventually periodic and so gets trapped very close to it's initial starting point.

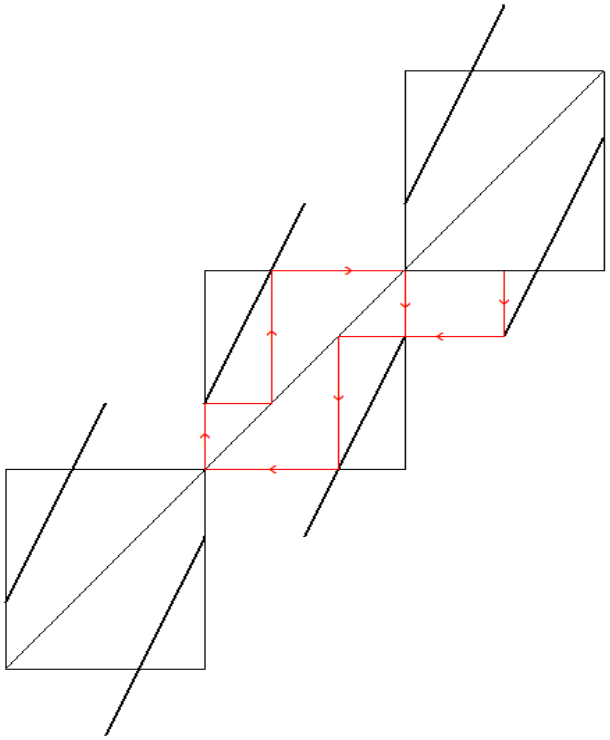

Figure 11: *The orbit of* $x = 0.5$ *for* $h = \frac{1}{3}$

To find the values of h that give us level 2 local minimums, we solve,

$$\tilde{M}_h^2(0.5) = \frac{1+h}{2} \quad . \tag{55}$$

We obtain two solutions to Eq.(55), for $\frac{1}{3} \leq h \leq \frac{1}{2}$ we get,

$$\begin{aligned} \tilde{M}_h^2(0.5) &= \frac{1+h}{2} \\ \tilde{M}_h(1-h) &= \frac{1+h}{2} \\ 2(1-h)-h &= \frac{1+h}{2} \\ h &= \frac{3}{7} \quad . \end{aligned} \tag{56}$$

For $0 \leq h \leq \frac{1}{3}$ we get,

$$\begin{aligned} \tilde{M}_h^2(0.5) &= \frac{1+h}{2} \\ \tilde{M}_h(1-h) &= \frac{1+h}{2} \\ 2(1-h)-1-h &= \frac{1+h}{2} \\ h &= \frac{1}{7} \quad . \end{aligned} \tag{57}$$

Eqs.(56,57) tell us that there are two values of h for which we get a level 2 local minimum. See Fig.(12) for the corresponding orbits of $x = 0.5$. The reason that the level 2 local minimums represent less distinctive minimums than the one at $h = \frac{1}{3}$ is due to the sensitive dependence on initial conditions of the map $M_h(x)$. Due to this, nearby orbits move apart at each iteration. We see that the periodic orbit at $h = \frac{1}{3}$ contains 4 iterations whilst the orbit at $h = \frac{3}{7}$ and $h = \frac{1}{7}$ contain 6 iterations. Therefore, more points will stay closer to the periodic orbit at $h = \frac{1}{3}$ for longer than at the values $h = \frac{3}{7}$ and $h = \frac{1}{7}$. Hence the periodic orbit displayed in Fig.(11) creates a more dramatic, distinctive local minimum than the ones depicted in Fig.(12). See Fig.(13) for an illustration. The same analysis is also true for the nature of the local maximums. For $h = 0.5$, the point $x = 0.5$ needs n iterations in order to get n boxes away from it's starting box, whilst for $h = \frac{1}{6}$, the point $x = 0.5$ needs $2n$ iterations. With more iterations comes more spreading out of an initial interval, so less points will travel along with the point $x = 0.5$. Hence the local maximums are less distinctive.

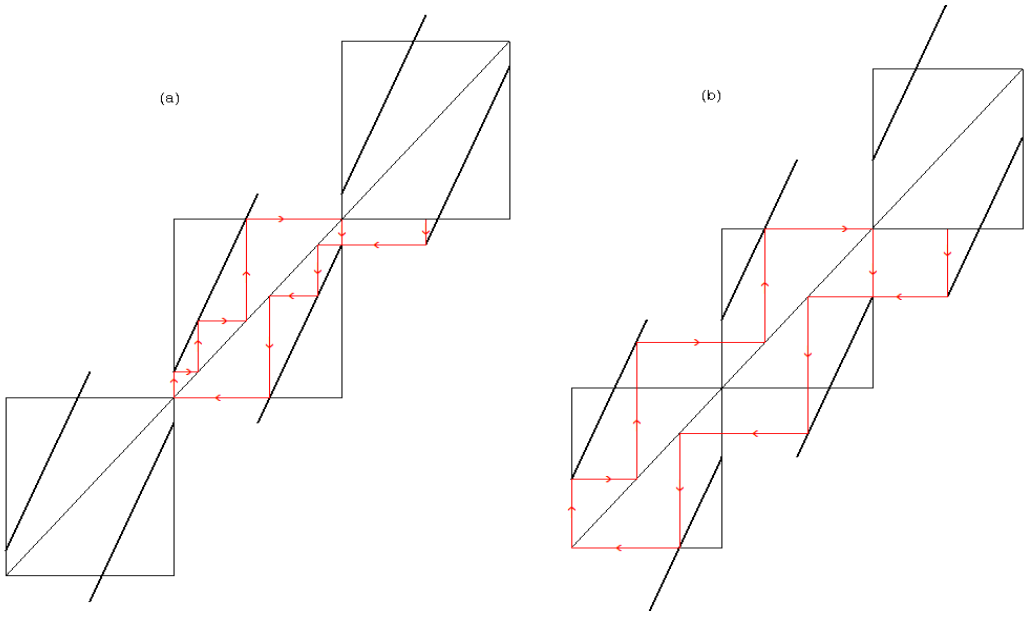

Figure 12: *Periodic orbits.* The orbits of $x = 0.5$ for $h = \frac{1}{7}$ in (a), and for $h = \frac{3}{7}$ in (b).

In general, the local maximums in the fractal region of the diffusion coefficient, are the solutions of,

$$\tilde{M}_h^n(0.5) = 0.5 \quad , \quad n \in N. \tag{58}$$

Similarly, the local minimums in the fractal region of the diffusion coefficient, are the solutions of,

$$\tilde{M}_h^n(0.5) = \frac{1+h}{2} \quad , \quad n \in N. \tag{59}$$

Where we solve for h. In general, if we evaluate $\tilde{M}_h(x)$ where x is rational, we obtain a rational value. In addition, we know that for $n = 1$ the solutions of Eq.(58) and Eq.(59) are rational. If we assume that $\forall m < n$, the solutions of Eq.(58) and Eq.(59) are rational, we can construct a simple inductive proof that all the solutions are rational values,

$$\begin{aligned} \tilde{M}_h^n(0.5) &= \tilde{M}_h\left(\tilde{M}_h^{n-1}(0.5)\right) \\ &= \tilde{M}_h\left(\frac{a}{b}\right), \quad a, b \in N. \\ &= \frac{c}{d} \quad c, d \in N. \end{aligned} \tag{60}$$

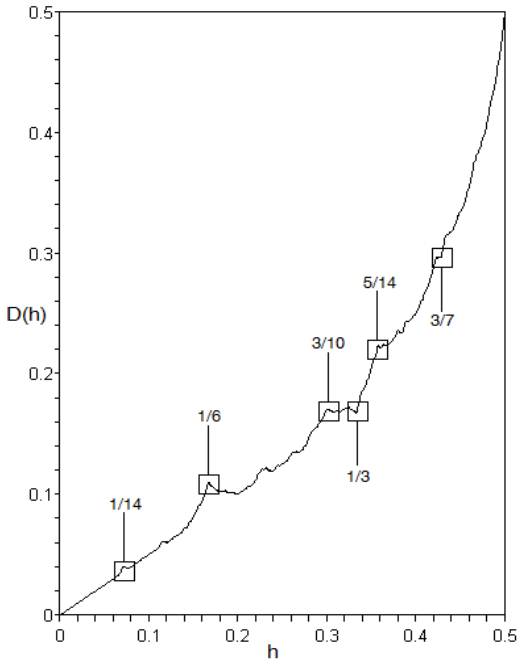

Figure 13: *Some of the very distinctive turning points in the fractal region of $D(h)$.* In this figure, the fractal region of $D(h)$ is depicted with some of the very distinctive turning points highlighted. These values of h have been calculated by defining different classes of Markov partition that give either highly diffusive behaviour for the local maximums, or restrict diffusion for the local minimums. (This image was created in *Maple 9.5*).

The result obtained in Eq.(60), means that the calculation of the extreme points is relatively simple. In other diffusive maps, the same method requires high order functions to be solved, and this quickly leads to irrational values as solutions, (see[7]). In addition Eq.(58) and Eq.(59), have another important consequence. A local extreme point can be defined for each value of n, hence there are an infinite amount of extreme points. This gives the diffusion coefficient it's fractal quality.

6 Conclusion

Deterministic diffusion has been studied in a lifted Bernoulli shift map. Starting from Einstein's formula for diffusion, the Taylor-Green-Kubo formula was derived. Using this formula, an exact, analytical expression has been found for the diffusion coefficient, in terms of the lift parameter, and Takagi functions. The method used required the use of an invariant density. In other cases, (see [7]), the invariant density is found to be parameter dependent. However, in our case, the invariant density was found to be a constant function. This helped simplify the analysis, and focused the dependence that the diffusion coefficient has on Takagi functions. The expression obtained for the diffusion coefficient is illuminating as it can be simplified to illustrate the global behaviour for small and large values of the parameter. For small values, the diffusion coefficient is composed of a linear part and a fractal Takagi function. For large values it is composed of a quadratic part, and a Takagi function. In order to explain the fractal nature of the diffusion coefficient, a method to evaluate the extrema, based on Markov partitions was used. It was found that all of these extrema are rational values. This makes their calculation simple relative to similar parameter dependent maps, (see [7]), in which irrational values are quickly encountered when employing the same method. Hence, this particular map is a very good example for studying deterministic diffusion and the diffusion coefficient.

For further study, one could introduce a bias parameter into the map, which would induce a current and we could study diffusion in this system. Due to the bias, the Takagi functions would no longer converge, and appropriate corrections would be needed. Theoretically, by moving the Taylor-Green-Kubo formula into the co-moving coordinate system of the ensemble, exactly the same diffusion coefficient should be recovered. The difficulty would be in finding the appropriate way to make the Takagi functions converge, so as to make the Taylor-Green-Kubo formula converge.

References

[1] Devaney, R.L. *An Introduction to Chaotic Dynamical Systems*. 2nd edn. (Westview Press, Boulder, 2003)

[2] Dorfman, J.R. *An Introduction to Chaos in Nonequilibrium Statistical Mechanics*. (Cambridge University Press, Cambridge, 1999).

[3] Gaspard, P. *Chaos, Scattering and Statistical Mechanics*. (Cambridge University Press, Cambridge, 1998).

[4] Gaspard, P and Klages, R. *Chaotic and Fractal Properties of Deterministic Diffusion-Reaction Processes*. Chaos, **8**, 409-423 (1998).

[5] Hilborn, R.C. *Chaos and Nonlinear Dynamics, An Introduction for Scientists and Engineers*. (Oxford University Press, New York, 1994)

[6] Klages, R and Korabel, N. *Understanding deterministic diffusion by correlated random walks*. J.Phys.A:Math.Gen, **35**, 4823-4836, (2002).

[7] Klages, R. *Deterministic Diffusion in One-Dimensional Chaotic Dynamical Systems*. Ph. D. thesis, Wissenschaft and Technik Verlag, Berlin, Germany, 1996.

[8] Klages, R. *Introduction to Dynamical Systems*. Lecture Notes for MAS424/MTHM021 Queen Mary, University of London, Version 1.2, 2008.

[9] Klages, R. *Microscopic Chaos, Fractals and Transport in Nonequilibrium Statistical Mechanics*. (World Scientific Publishing, Singapore, 2007)

[10] Lasota, A. and Mackey, C. *Chaos, Fractals and Noise. Stochastic Aspects of Dynamics. (Applied Mathematical Sciences vol 97)*. 2nd edn. (Springer, Berlin, 1994)

[11] Reif, F. *Fundamentals of Statistical and Thermal Physics*. (McGraw-Hill, Singapore, 1985)

[12] Schuster, H.G. *Deterministic Chaos. An Introduction*. (Physik-Verlag, Weinheim, 1984).

[13] Wax, N (ed). *Selected Papers on Noise and Stochastic Processes*. (Dover, New York, 1954). See Kac, M. *Random Walk and the Theory of Brownian Motion*.